Microchimica Acta (2020) 187:585
https://doi.org/10.1007/s00604-020-04503-4

ORIGINAL PAPER

Microfluidic electrochemical immunosensor for the determination of cystatin C in human serum

K. S. Shalini Devi[1,2] · Uma Maheswari Krishnan[1,2,3]

Received: 9 March 2020 / Accepted: 18 August 2020

Abstract

The fabrication of a nanointerfaced electrochemical immunosensor is described for the rapid determination of cystatin C, a biomarker that is elevated in diabetic retinopathy. A dispersion of graphene oxide-chitosan (GO-Chit) nanocomposite was used to modify the carbon working electrode, allowing for a high conjugation of anti–cystatin C antibody. This modified sensor was characterized both morphologically and electrochemically, and the sensor performance was evaluated towards selective quantification of cystatin C in simulated as well as serum samples using cyclic voltammetry and differential pulse voltammetry. The sensor was able to detect cystatin C in the concentration range1 - 10 mg/L with a detection limit of 0.0078 mg/L. The preparation time of the sensor was 420 s, which was faster than that of conventional ELISA and other electrochemical sensors reported in literature. The clinical applicability of the proposed electrochemical biosensor was demonstrated through quantification of cystatin C in human serum samples and identification of diabetic retinopathy. A cutoff value of 1.2 mg/L of cystatin C was used beyond which the samples were classified as positive for diabetic retinopathy. Two different working electrodes, namely a glassy carbon electrode (GCE) and paper electrodes, were used in the study. The working potential was set to 0.25 V vs. Ag/AgCl for experiments with the GCE and 0.15 V for the paper electrodes. The prediction was validated by clinical diagnosis wherein the prediction accuracy of the sensor exceeded 85%. The sensor platform was translated onto a paper substrate and characterized for achieving an optimum sensing performance. This work is the first attempt to employ an electrochemical cystatin C sensor for the diagnosis of diabetic retinopathy from serum samples.

Keywords Cystatin C · Immunosensor · Diabetic retinopathy · Electrochemical detection · ELISA

Introduction

Over the years, there has been an increasing incidence of diabetic retinopathy (DR) in Indian population due to high blood pressure, smoking and alcohol consumption, time since onset of diabetes, ethnicity, gestational diabetes, and serum lipid levels in an individual. Despite several biomarkers indicated for diagnosis, detection of such markers with utmost sensitivity still remains largely underexplored. In recent years, clinicians have identified cystatin C (Cys C) to be a reliable marker for the diagnosis of diabetic retinopathy [1]. A serum concentration of Cys C > 1.12 mg/L implies a 3-fold greater risk of moderate DR [2]. Human Cys C is a basic 13-kDa protein with 120 amino acid residues present in a single polypeptide chain. It is also referred to as "post γ-protein" containing a 26–amino acid leader peptide [3]. The normal concentration range of Cys C in human body fluids (serum and urine) in males and females was found to be 0.51–0.98 mg/L [4]. Recently, abnormally elevated levels of Cys C have been identified as a prognostic marker for various diseases including neurodegenerative diseases, cardiovascular disorders, and cancer [5]. Higher levels of Cys C in serum have also been correlated to polycystic ovarian syndrome (PCOS) and endocrine disorders [6]. A recent report demonstrates that Cys C,

Electronic supplementary material The online version of this article (https://doi.org/10.1007/s00604-020-04503-4) contains supplementary material, which is available to authorized users.

✉ Uma Maheswari Krishnan
umakrishnan@sastra.edu

[1] Centre for Nanotechnology and Advanced Biomaterials (CeNTAB), SASTRA Deemed-to-be University, Thanjavur, Tamil Nadu 613401, India

[2] School of Chemical and Biotechnology, SASTRA Deemed University, Thanjavur 613401, India

[3] School of Arts, Science and Humanities, SASTRA Deemed University, Thanjavur 613401, India

Published online: 30 September 2020

being a protease inhibitor, acts as a potential indicator for tubular damage and impaired renal function involved in chronic kidney disease (CKD) [7].

Traditional methods of Cys C detection employed thus far include the automated particle-enhanced turbidimetric immunoassay (PETIA) [8], which is the first automated assay used for the detection of Cys C with a throughput of 90 samples per hour and less than 10 min for a sample; enzyme-linked immunosorbent assay (ELISA) [9]; particle-enhanced nephelometric immunoassay (PENIA); sol-particle immunoassay (SPIA) [10]; hybridization chain reaction (HCR); and DNA-based and rolling circle amplifications [11]. Unfortunately, all these techniques involve tedious laboratory preparations, a large number of sample volumes as electrolyte solutions, skilled personnel, and expensive chemicals and devour a huge expense of time besides generating false-positive results during colouration and employment of carcinogenic chemicals like ethidium bromide. In order to circumvent these drawbacks, electrochemical biosensors can be employed for the quantification of Cys C. A scan of literature reveals very few attempts to fabricate electrochemical sensors for Cys C determination. None of these electrochemical sensors has used Cys C levels to diagnose DR; instead, most of these sensors have looked as Cys C as a diagnostic marker for renal disorders. An electrochemical biosensor developed for determining Cys C levels in chronic kidney disease (CKD) used papain enzyme immobilized on disposable nanotube-modified commercial screen-printed carbon-based electrode (SPMWE-COOH) [12]. The sensor exhibited a response of 10 min for the detection of Cys C in the concentration range of 0.6×10^{-5}–0.6×10^{-2} ng μL^{-1}. A ferrocene-graphene blend was used to modify the working electrode and incorporate anti–Cys C on a gold working electrode. This immunosensor reported a detection range of 0.1 to 1000 ng/mL and a detection limit of 0.03 ng/mL [13]. Several other reports have employed glassy carbon electrode modified with DNA [14], titania nanotubes [15], multiwalled carbon nanotubes, and immunopillar chips [16]. These attempts were slow and expensive and have not explored the use of these sensors for the diagnosis of DR. Based on the opportunities available in this domain, we aim to develop an electrochemical biosensor for the detection of Cys C in diabetic patients (age above 35 years) to quantify Cys C from serum and use these values for the diagnosis of diabetic retinopathy. Owing to their defined structure, high surface area, biocompatibility, and electrical conductance, graphene/graphene oxide–based materials have been widely utilized for electrochemical biosensor applications [17–19]. Among the various graphitic nanomaterials, the functional group present on the edges of graphene oxide (GO) is well-suited for clasping the biomolecules firmly. Initially, we have characterized electrochemically the graphene oxide-chitosan (GO + Chit) nanocomposite, using the benchmark redox mediator ferricyanide $[Fe(CN)_6]^{3-}$, and the highly specific and selective anti–cystatin C antibody (anti–Cys C) was used as a Cys C capturing agent. The Cys C values were quantified in serum samples and used to diagnose diabetic retinopathy. Finally, the electrode modifications were translated on a paper electrode integrated with a microfluidic platform for the portable and affordable screening of individuals.

Materials and methods

Chemicals and reagents

Cystatin C (Cys C) monoclonal and polyclonal antibody was purchased from R&D Systems, USA. Graphene oxide (GO) (> 80% carbon with flake dimensions of 0.5–2.0 μm and thickness of 0.6–1.2 nm), chitosan flakes (low molecular weight), 1-ethyl-3-(3-dimethyl-aminopropyl) carbodiimide (EDC) and *N*-hydroxysuccinimide (NHS), and Tween 20 were obtained from Sigma-Aldrich Chemicals, USA. Potassium hexacyanoferrate (III) $[K_3Fe(CN_6)]$, sodium dihydrogen phosphate, disodium hydrogen phosphate, ethanol, paraffin wax (Merck, India), and other chemicals used in the study were of analytical grade and used without additional purification. The supporting electrolyte used throughout the work was phosphate buffer solution (PBS) of pH 7 and ionic strength = 0.1 mol L^{-1}. Polydimethylsiloxane (PDMS) and its curing agent were purchased from SYLGARD (DC/GEN/184, 1.1 kg silicone elastomer kit).

Instrumentation

Voltammetric measurements were performed with a CHI6013C instrument (CH Instruments, USA) and Dropsens from Metrohm India Limited. Three-electrode configurations consisting of glassy carbon electrode (GCE) and its chemically modified system ($0.0707 cm^2$) as a working electrode, Ag/AgCl (3 M KCl), and platinum were employed as reference and counter electrodes respectively for the quantification of the analyte. Scanning electron microscopy (SEM) was performed using TESCAN Vega, Czech Republic. Electrochemical impedance analysis was performed using a CHI604C instrument, USA. All electrochemical measurements were recorded at room temperature.

Atomic force microscopy (Model No.: 5100, Agilent Technologies, USA) was used to study the topographical changes at each stage of modification of the working electrode. AFM images of the bare electrode followed by the antibody immobilization on the modified electrode were sequentially analyzed by monitoring the roughness parameter using the Gwyddion software. AFM images were then processed to calculate the roughness, maximum height, and the depth of the modification.

Preparation of the screen-printed paper electrodes

Screen-printed wax-coated paper electrodes (SPEs), with 4-mm-diameter working area, were fabricated in-house using suitable OHP stencil designs. For each fabricated electrode, a carbon ink formulation (Product Code: 124-50; Creative Materials Inc., USA) was initially screen-printed on a wax-coated paper (250 μm thickness) and served as the electrode material for both working and counter electrodes. After curing the carbon layer at room temperature for 30 min, the silver reference electrode was screen-printed using electrically conductive Ag/AgCl paste (Product Code; 120-07, Creative Materials Inc., USA) over the wax-coated substrate, which was subsequently cured at ambient conditions for 30 min. The prepared electrode was made compatible with the μSTAT4000 screen-printed cable (CAST110) from Dropsens.

Preparation of the biosensor

Preparation of the GO-Chit nanocomposite

The GO stock was prepared by dispersing the commercially received 3 mg of GO in 1 mL ethanol. The chitosan stock solution was prepared by mixing 50 mg chitosan (Chit) flakes with 1% glacial acetic acid (10 mL) and stirred at room temperature for 3 h to achieve a clear solution. The pH was made to 4–5 using a ~ 0.1 M NaOH solution. A mixture consisting of 250 μL of GO-ethanol suspension and 250 μL of Chit-acetic acid solutions was subjected for 15 ± 2 min sonication to form a homogenous GO-Chit dispersion.

Fabrication of the immunosensor

About 5 μL of GO-Chit was drop-cast on the pre-cleaned GCE and air-dried for 5 ± 1 min at room temperature (25 ± 2 °C). Next, for the amidation, the GCE/GO-Chit electrode was treated with 1:1 v/v ratio of EDC-NHS (10 mM of each in 10 mL of phosphate-buffered saline, pH 7) [20] followed by drop-casting of 5 μL of anti–cystatin C antibody (100 μg/mL) and dried for 5 min at room temperature to get GCE/GO-Chit/anti–Cys C [21]. After immobilization of the antibody, the electrode was incubated with bovine serum albumin (BSA) 5% (w/v) (5 mg mL^{-1}) for 2–5 min to block non-specific binding sites. Finally, the fabricated electrode was designated as GCE/GO-Chit/anti–Cys C. A label-free approach was adopted for cystatin C detection in the first set of trials in the conventional system. The redox mediator ferricyanide $[Fe(CN)_6]^{3-}$ was utilized for the electron transfer studies. The same set of experiments was conducted at the SPE working area with 4 mm diameter as followed on GCE for real-time analysis. Scheme 1 shows the steps involved in the electrode fabrication. The different stages of modifications were characterized using electrochemical impedance spectroscopy (EIS), SEM, and AFM.

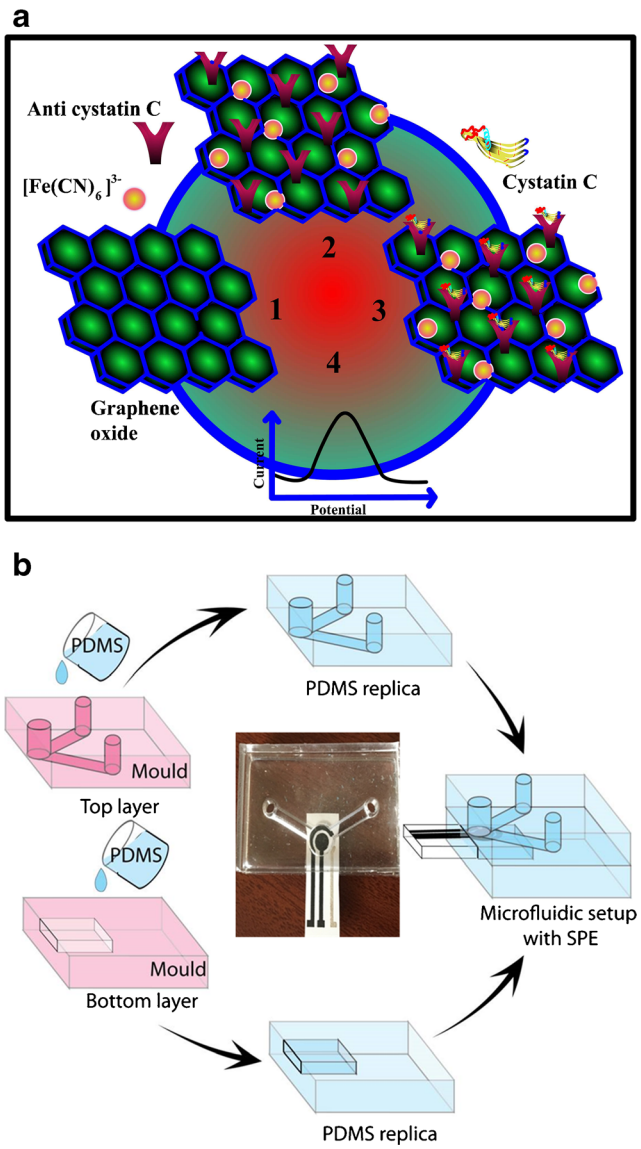

Scheme 1 (A) Development of the electrochemical immunosensor for cystatin C by sequential modification of GCE as well as SPE with GO/chitosan and loading of $Fe(CN)_6$ (step 1) and functionalization of electrode using EDC-NHS, anti–cystatin C modification (step 2). Blocking with bovine serum albumin (step 3), and mechanism involved in the electrocatalytic reaction of cystatin C. Step 4 is the pictorial representation of electrochemical pulse signal. (B) Overall schematic representation of the microfluidic channel with the screen-printed paper-based electrode. Actual picture of the microfluidic chamber with the screen-printed electrode is shown in the centre of the scheme

ELISA protocol for real-time samples

Multianalyte ELISA kit (R&D from Biologix) was used to detect the levels of cystatin in the serum collected from the volunteers. Following the manufacturer's protocol, 50 μL of serum samples was collected from patients and diluted to 1:2000 after optimization of the dilution ratio. The samples were incubated for 2 h at room temperature. After 2 h, detection antibody solution (100 μL) was added and incubated for

1 h. Followed by incubation, the strips were washed 4 times using the washing buffer and 100 μL avidin-HRP solution was added and incubated for 30 min at room temperature. After washing, development solution (100 μL) was added to each well and incubated for 15 min at room temperature in the dark. Then, 100 μL of stop solution was added to stop the reaction and the absorbance of the samples was measured at a wavelength of 450 nm using a multimode reader (BioTek Epoch ELISA reader).

Collection of samples for real-time analysis

Serum was isolated from blood samples obtained from healthy volunteers and diabetic patients by the clinicians from the hospital by centrifugation. The samples collected conveyed a positive response and control behaviour towards cystatin C initially confirmed by the ELISA technique by the technicians, and the tested samples were stored in a refrigerator. About 5 μL of an unknown serum sample was added without any further dilution to the modified electrode dipped in the buffer solution (pH 7 PBS, 10 mL for GCE sensor and 195 μL for the paper electrode). The current was recorded using differential pulse voltammetry (DPV) after addition of the sample, and the concentration of cystatin C was determined from the standard plot. The values from the developed sensor were compared with the actual samples as well as the ELISA analysis and tabulated. Ten different samples were obtained for validation of the sensor after the ethical approval from RCUK council. The recovery studies were also performed in serum samples by the standard addition method. The cystatin levels were measured using the developed sensor after each addition of known quantities of cystatin C.

Preparation of microfluidic model with 3D printing mould

The mould was designed using the SolidWorks® software and 3D-printed using ABS (poly(acrylonitrile-*co*-butadiene-*co*-styrene) and PolyJet filament in the Stratasys Objet 260 Connex 3 printer. The mould was used to cast PDMS in two parts. The top layer of the mould was fabricated to hold 100 μL volume containing inlet and outlet, and the bottom layer was designed with 0.5 mm depth for placing the SPE. PDMS polymer was mixed with its curing agent in the ratio of 1:10 (10 mL of PDMS in 1 mL of curing agent). The prepared mixture was poured into the 3D-printed mould and the bubbles were allowed to settle down for about 10 min. Then, the mould was dried in a microwave oven for about 5 min at 400 °C. The two layers of silicone were then peeled off using forceps and then placed in contact with each other in proper alignment. The paper electrode was placed in the slot provided, and the system was checked for ensuring blockage-free and leakage-free flow of the sample. Scheme 1A depicts the stages involved in the fabrication of the microfluidic chamber.

Results and Discussion

Physicochemical characterization

SEM of the SPE/GO-Chit@anti–Cys C

Morphological changes after modifying the screen-printed electrodes after each step were monitored using a scanning electron microscope (SEM), and the images are presented in Fig. 1. The scanning electron micrographs reveal the ultrafine carbon particles on the bare electrode surface. On introduction of the GO/Chit layer, larger flakes of GO are visible on the electrode surface. The covalent modification with anti–cystatin C antibody increases the size of the particles distributed on the surface as well as the charging on the surface suggesting the presence of an additional insulating layer on the surface.

AFM analysis of SPE/GO-Chit/anti–Cys C@Cys C

The AFM analysis of the surface topography of the paper electrodes after various stages of modifications reveals a progressive increase in the average roughness (R_a) values from 11.16 nm ± 0.02 (maximum height: 144.2 nm) for bare GCE to 14.6 nm (maximum height: 198.5 nm) for GCE/GO-Chit and 19.3 nm (maximum height: 388.4 nm) for GCE/GO-Chit-anti–Cys C, indicating the successive additions of layers on the GCE (Supplementary Fig. S1). When cystatin C was added to this electrode, the R_a value further increased to 20.97 nm (maximum height: 742.2 nm) that indicates the successful capture of the target analyte Cys C by the antibody-modified surface [22]. Additional information of other parameters supporting the results has been tabulated in Supporting Table S1.

FTIR characterization

FTIR spectra of GO, chitosan, GO-Chit, and GO-Chit-anti–Cys C were analyzed to confirm composite formation and antibody binding by identifying the functional groups involved. The FTIR spectrum of chitosan shown in Fig. 2A reveals a broad -O-H vibrational band at 3433 cm^{-1} and -C-H stretching vibrations at 2922 cm^{-1}. A medium intensity -N-H bend is observed at 1658 cm^{-1} while the C-H bend is seen at 1377 cm^{-1}. The -C-O vibrational band is observed at 1077 cm^{-1}. The spectrum of GO (Fig. 2B) shows a band at 3389 cm^{-1} that may be attributed to the -O-H stretch. A weak band appears at 1716 cm^{-1} due to the carbonyl stretch of carboxylic acid functionalities. The band at 1571 cm^{-1}corresponds to sp^2 C=C stretching, and the C-OH

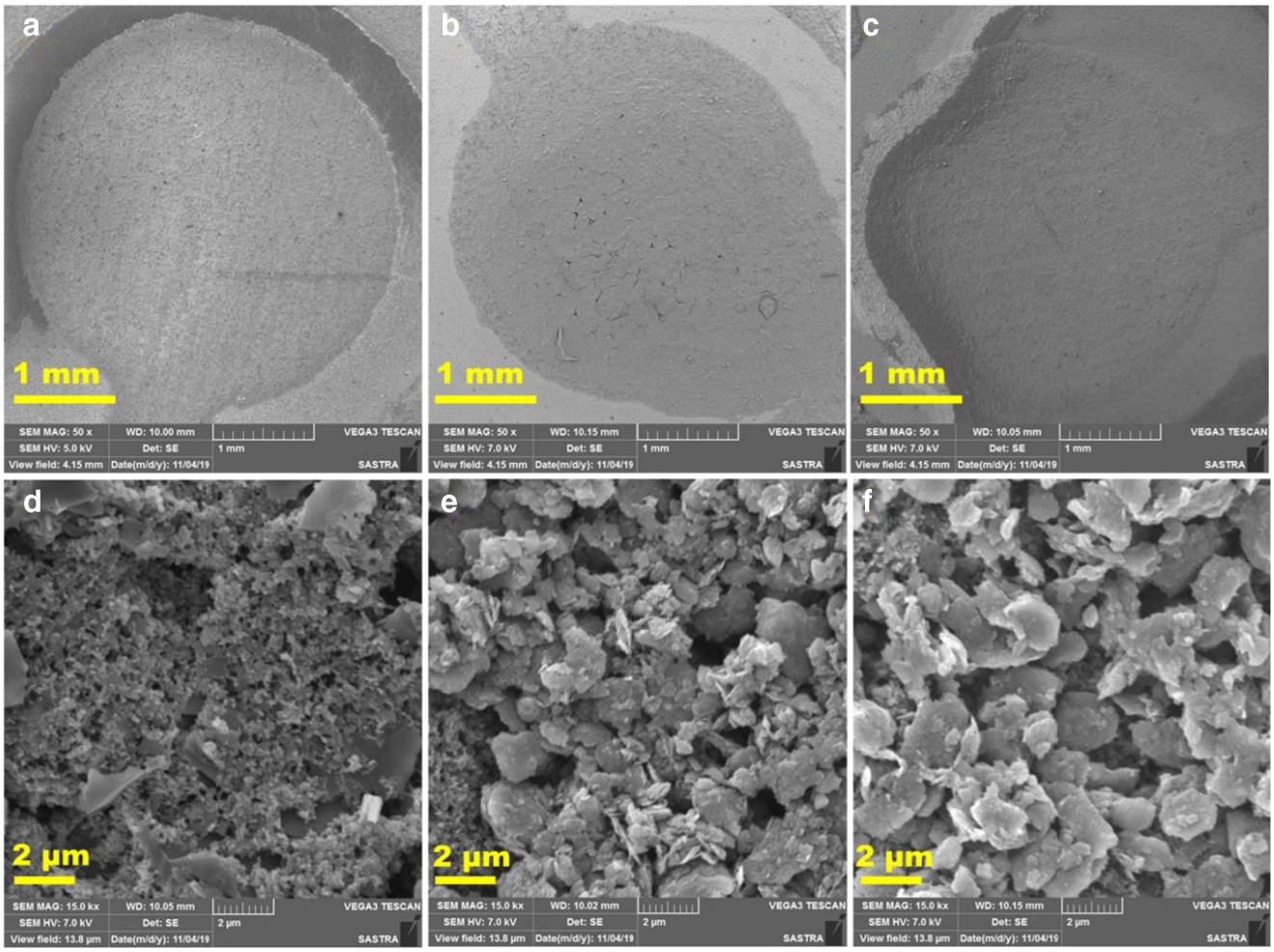

Fig. 1 SEM images of the bare screen-printed paper electrode (A, D), GO-Chit coated on the screen-printed paper (B, E), and anti–Cys C modified with GO-Chit on the paper substrate (C, F)

vibration appears at 1423 cm^{-1} as a low intensity band [23]. It may be inferred from the FTIR spectrum that the GO contains carboxylic functional groups at the edges of the graphene plane. The mixture of GO and chitosan retains the 1574 cm^{-1} (C=C stretch) of GO and exhibits the characteristic vibration bands of chitosan at 3422 cm^{-1} (-O-H stretch), 2871 cm^{-1}(-C-H stretch), 1657 cm^{-1} (-N-H bend), 1381 cm^{-1} (-C-H bend), and 1078 cm^{-1} (-C-O- vibration) [24, 25]. The slight negative shift of the -O-H stretching frequency of chitosan in the chitosan-GO composite (GO-Chit) indicates the non-covalent interactions between chitosan and GO. The FTIR spectrum of anti–Cys C layered on the surface of modified GO-Chit reveals characteristic vibrational frequencies at 3736 cm^{-1} and 3433 cm^{-1} (-O-H stretch) and 2925 and 2853 cm^{-1} (-C-H stretch) due to chitosan. The band at 1637 cm^{-1} arises due to the carbonyl stretch of the amide functionalities present in the antibody. The low intensity band at 1557 cm^{-1} appears due to the GO component in the composite [26]. The bands at 1460 (-C=C stretch); 1377 (-C-H bend); 1322 cm^{-1} (-C-N stretch); 1153, 1078, and 1115.3 cm^{-1} (C-O stretching vibrations); and 599 and 593 cm^{-1} arise due to N-H amine groups in chitosan and antibody. A band at 1750 cm^{-1} in the FTIR spectrum of the GO-chitosan-anti–Cys C composite may be attributed to the covalent linkage between the carboxylic acid functionalities in GO and the antibody formed using the EDC-NHS chemistry.

Electrochemical measurements of GCE/GO-Chit-anti–Cys C

To evaluate the sensing performance of the fabricated sensor, ferricyanide, which possesses efficient anodic and cathodic peaks, was employed as a stand-alone mediator with 0.1 M PBS (pH 7) as supporting electrolyte. The cyclic voltammograms for the bare GCE and GO-Chit-modified GCE in the presence of $[Fe(CN)_6]^{3-}$ are shown in Fig. 3A. The cyclic voltammograms display the typical redox peak of the ferro-ferricyanide redox couple at 0.29 V vs Ag/AgCl. The redox peak current increases

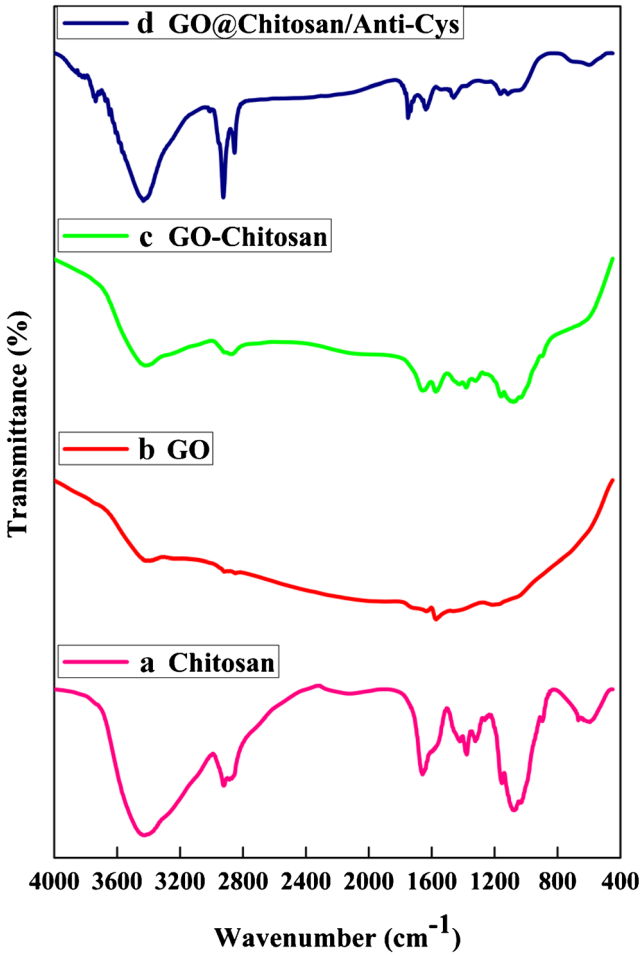

Fig. 2 FTIR spectra of (A) chitosan, (B) GO, (C) GO-chitosan (GO-Chit), and (D) GO-Chit-anti–Cys C

by 15 μA in the GO-Chit/GCE electrode when compared with that in the bare GCE. This increase may be attributed to the presence of the GO and the polar chitosan which increases the active surface area for better electron transfer. Previous reports have indicated that GO easily forms complexes with cationic species and hence the mixture of GO and chitosan forms a stable hydrophilic layer on the GCE surface [27]. The electrostatic attraction between the positively charged amino moieties of chitosan (pKa ~ 6.4) and negatively charged ferricyanide favours better electron transfer that is observed from the higher current flow in the GO-Chit-modified electrode. Conjugation of the anti–Cys C antibody on the GO-Chit composite resulted in a significant increment in the peak current by 19 μA which represents a 134% increase from the peak current obtained in the bare GCE. The amine groups of the chitosan layer favour the binding of antibody on the electrode surface through formation of amide links. The redox peak potential shows no shift in the modified electrodes. This interface can, therefore, be useful for the sensitive detection of the analyte. When the target analyte cystatin C was added to the modified working electrode (GCE/GO-Chit-anti–Cys C), it showed an electrocatalytic reduction at 0.31 V vs Ag/AgCl when the voltage was scanned at a rate of 10 mV s^{-1}. Further addition of cystatin C was accompanied by a concomitant decrease in the peak current due to the formation of the immune complex that retards the diffusion of the electroactive species. This set of experiments demonstrated that the immunosensor could detect the presence of cystatin C in the sample.

The cyclic voltammetric response of the various scan rates of the modified electrodes GCE/GO-Chit and GCE/GO-Chit-anti–Cys C in $[Fe(CN)_6]^{3-}$ containing electrolyte showed a progressive increase in both anodic and cathodic peak currents (Fig. 3B) with increasing scan rates. A baseline corrected plot of peak currents which consists of i_{pa} and i_{pc} against the scan rate (v) for the modified electrode (GO-Chit-anti–cystatin C) showed a linear trend from the origin, showing a surface-confined electron transfer mechanism in the system (Fig. 3C). This indicates that $[Fe(CN)_6]^{3-}$ serves as an effective electron-transfer shuttle in the system [28]. The surface concentration of the electroactive ferricyanide couple (Γ, mol cm^{-2}) in GCE/GO-Chit can be determined from the slope value of the peak current vs scan rate (Fig. 3B). In general, the peak current of a reversible reaction is given by the following equation:

$$i_{pa} \text{or} i_{pc} = n^2 F^2 A \Gamma v \quad (1)$$

where n denotes the number of electrons transferred, F represents the Faraday constant (96,500), A denotes the geometrical area of the electrode (0.0707 cm^2), and v is the potential scan rate [29]. The active surface area calculated using the above equation was found to be 4.39×10^{-10} mol cm^{-2}, 6.89×10^{-10} mol cm^{-2}, and 10.56×10^{-10} mol cm^{-2} for the bare GCE, GCE/GO-Chit electrode, and GCE/GO-Chit/anti–Cys C–modified electrode, respectively.

The electron transfer at the electrode-electrolyte interface was investigated using the modified GCE/GO-Chit/anti–Cys C electrode through differential pulse voltammetry (DPV), which is a more sensitive technique than cyclic voltammetry [30, 31]. As a control, optimization of important measurement parameters is shown for the pre-modification step potential fixed at 0.2 V vs Ag/AgCl while amplitude, pulse width, sampling width, and increment E_{step} were varied. The results are shown in Supplementary Fig. 3A–C. The highest values obtained were chosen as optimum in each case. The optimum amplitude and pulse widths were 0.1 s and 0.02 s, respectively. In the case of increment E_{step} and sampling width, no significant changes were observed, and hence, the highest sampling width value of 0.005 s was chosen in both cases for further trials.

The calibration plot for electrochemical immunosensing of cystatin C was obtained by recording the electrochemical response of the GCE/GO-Chit/anti–Cys C–modified electrode at pH 7 on addition of

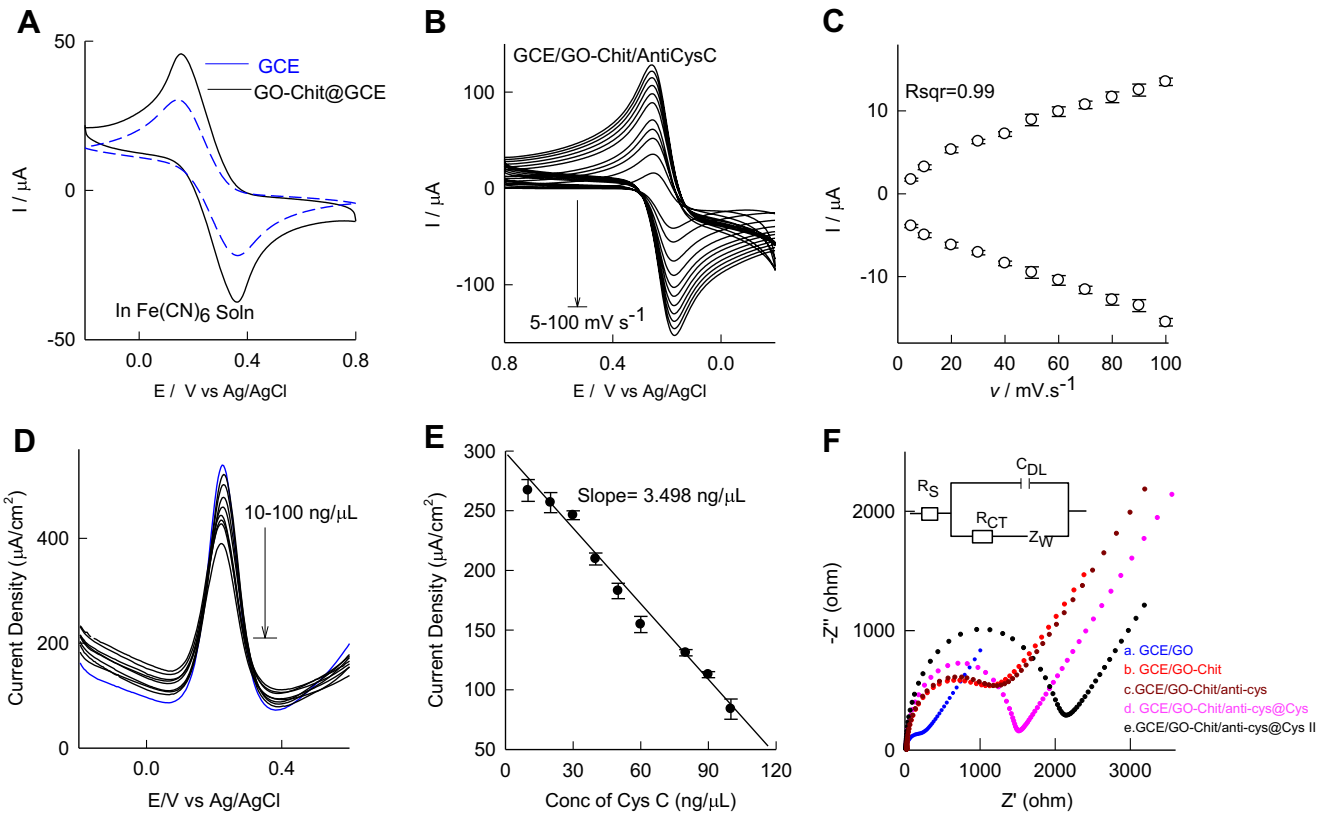

Fig. 3 Electrochemical CV response of 5 mM $Fe(CN)_6$ in pH 7 PBS on bare GCE and GO-Chit-modified GCE (A). GCE/GO-Chit/anti–Cys C at different scan rates from 5 mV to 100 mV s^{-1} (B, C). The plot of scan rate (v) and its respective current response of the modified electrode in $Fe(CN)_6$ dissolved in pH 7 PBS solution. DPV of concentration effect of modified electrode, i.e. GCE/GO-Chit@anti–Cys C with the ten different concentrations from 1 to 10 mg/L (D) and its calibration plot of concentration vs current (E). Impedimetric responses of the (a) GCE/GO, (b) GCE/GO-Chit, (c) GCE/GO-Chit@anti-Cys, (d) GCE/GO-Chit/anti-Cys@Cys I, and (e) GCE/GO-Chit/anti-Cys@Cys II. Inset is the pictorial representation of the Randles circuit model (F)

different concentrations of cystatin C sequentially. Figure 3D shows the typical calibration response for cystatin C obtained using different dilutions (1–10 mg L^{-1}). The sensor showed a progressive reduction in the current on the addition of cystatin C. A linear response was obtained between the concentration ranges of 10–100 ng μL^{-1} (Fig. 3E). The limit of detection (LOD) has been calculated using the formula in equation with $S/N = 3$.

$$\mathrm{LOD} = 3S_b/m \quad (2)$$

where S_b is the standard deviation obtained from five measurements of the blank signal. The clinically relevant concentrations of cystatin C for the diagnosis of diabetic retinopathy are above 1.2 mg/L.

EIS measurements

To investigate the interfacial properties between the electrode and electrolyte surface after different electrode modifications, electrochemical impedance spectroscopy (EIS) was performed. Figure 3F shows the EIS responses of bare GCE and different surface modified GCE in a bath solution containing 5 mM $[Fe(CN)_6]^{3-}$ dissolved in PBS (pH 7) at an applied potential of 300 mV vs Ag/AgCl. The pattern obtained in the EIS can be attributed to the charge transfer reaction (R_{CT}) as well as the diffusion of the analyte [32]. The Randles equivalent circuit where the solution resistance (R_s) and double-layer capacitance (C_{dl}) are arranged in parallel with charge transfer resistance (R_{ct}) and Warburg resistance (Z_w), was used to calculate the R_{CT} values (Fig. 3F inset). Among these elements, the R_{ct} is the most sensitive parameter that responds to changes on the electrode interface [33]. The calculated R_{ct} value for GCE/GO is 60 Ω which increases by 20-fold to 1160 Ω for GO-Chit. Chitosan being an insulator contributes to the increase in impedance values by hindering the surface electron transfer. The introduction of the anti–Cys C antibody did not change the R_{CT} value significantly and was calculated to be 1168 Ω which was similar to the values obtained for GO-Chit. This suggests that the antibody-modified surface presents a similar barrier as chitosan to the surface electron transfer capability of GCE. On addition of 1 mg/L of cystatin C, the R_{CT} values

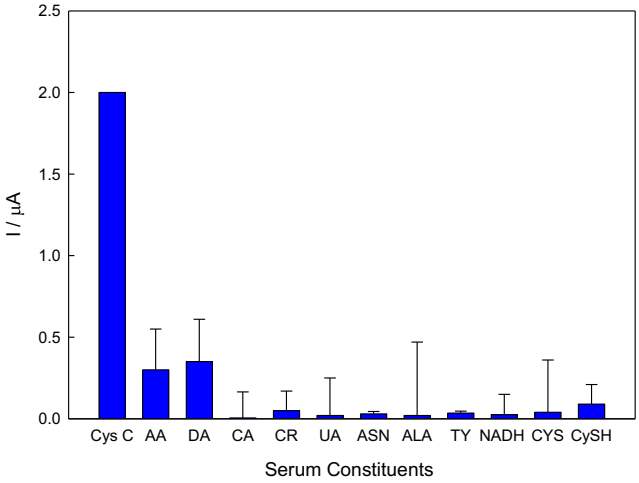

Fig. 4 Selectivity test with serum constituents, namely ascorbic acid, dopamine, citric acid, creatinine, uric acid, asparagine, alanine, tyrosine, nicotinamide adenine dinucleotide, and cystine along with cystatin C using the modified electrode GO-Chit/anti–Cys C

were found to increase to 1420 Ω, indicating the successful capture of the target analyte Cys C on the GO-Chit-anti–Cys C surface. The additional non-conducting layer formed by cystatin C contributes to the increase in the R_{CT} values. Further addition of 2 mg/L of cystatin C resulted in a corresponding increase in the R_{CT} values to 2100 Ω due to the increase in the non-conducting layer. Taken together, the FTIR spectroscopy and EIS results provide chemical and functional confirmation of the presence of anti–Cys C on the GO-Chit layer on GCE.

In order to monitor the specificity and storage stability of the modified GO-Chit-anti-Cys electrode, the following experiments were carried out. The possible interferents such as ascorbic acid (AA), citric acid (CA), creatinine (CR), uric acid (UA), asparagine (Asn), alanine (ALA), tyrosine (TY), nicotinamide adenine dinucleotide (NADH), cysteine (CysH), and cystine (Cys) commonly encountered in human serum samples were introduced in the bath solution, and the electrochemical measurements were recorded using the GO-Chit-anti–Cys C electrode along with Cys C [34]. DPV being a sensitive technique was employed to check the specificity of the sensor. The difference in the peak current (I_p) for Cys C and after addition of other interferent molecules was used to study the response of the modified electrode towards the interfering chemicals at the same potential. The concentration of the interferents used in the study was the same as that of Cys C (1 mg/L). The sensor was found to show excellent specificity towards the target Cys C, but AA showed a slight interference as an oxidizing analyte for the same electrode with a shift (20%) in the peak potential. No other interferents exhibited a change in the current (Fig. 4). This observation clearly indicates the selective electrochemical interaction of Cys C at the modified electrode. The reproducibility and the electrode stability of the GO-Chit/anti–Cys C sensor were studied by calculating the difference in DPV current recorded at regular intervals using the same electrode that was stored after use at 4 °C. The variation in peak current for three repeated measurements using the same electrode was found to be below 15%, indicating that the electrode could be used for at least 3 times. However, as the intended application of the electrode is to screen human serum samples, reuse of the same electrode may not be a prime requisite.

To investigate the real application of the fabricated electrochemical biosensor in clinical measurements for DR, the GO-Chit-anti-Cys-modified electrode was utilized to detect Cys C in human serum samples and to predict the patient's nature. The serum sample was diluted 10-fold with 0.1 M PBS (pH 7). The accuracy of Cys C determination was evaluated

Table 1 Real sample analysis compared with the ELISA technique

Sample no.	Measured current (µA)	Calculated value from the sensor (mg/L)	Prediction from t he sensor	Actual sample category	ELISA values obtained (mg/L)	Prediction based on ELISA
1.	8.12 ± 0.05	2.300 ± 0.2	DR	PDR	1.78	DR
2.	3.20 ± 0.05	0.914 ± 0.2	Normal	Control	1.60	DR
3.	4.40 ± 0.05	1.257 ± 0.2	Borderline DR	NPDR	1.31	DR
4.	8.00 ± 0.05	2.280 ± 0.2	DR	DM no DR	1.22	DR
5.	3.00 ± 0.05	0.857 ± 0.2	Normal	Control	1.49	DR
6.	10.00 ± 0.05	2.858 ± 0.2	DR	PDR	2.25	DR
7.	4.60 ± 0.05	1.310 ± 0.2	Borderline DR	NPDR	1.69	DR
8.	17.00 ± 0.05	4.850 ± 0.2	DM no DR	PDR	1.36	DR
9.	1.90 ± 0.05	0.543 ± 0.2	Normal	Control	0.042	Control
10.	10.60 ± 0.05	0.910 ± 0.2	Normal	Control	1.18	Control
Prediction accuracy (%)			80%			70%

Cystatin C greater than 1.2 mg/L was considered positive for DR

DR diabetic retinopathy, *PDR* proliferative diabetic retinopathy, *NPDR* non-proliferative diabetic retinopathy, *Control* normal healthy samples

Table 2 Comparison of different modified electrodes for the detection of cystatin C and its electrochemical parameters

Electrode	Technique	Linear range	Detection limit	Preparation time (s)	Sample	Disease diagnosed	Ref.
Micro immunopillar chip	ELISA	0–50 ng mL^{-1}	1 ng L^{-1}	1200	-	CKD in cats	[35]
Hairpin DNA–modified Au@Fe3O4 electrode	Electrochemical aptasensor	0.01 pg mL^{-1} to 30 ng mL^{-1}	3 fg mL^{-1}	7200	Human serum	CKD	[11]
μUNPD	Luminex assay	0.1 ng/mL and 20 ng/mL	0.1 ng mL^{-1}	6600	Human urine	CKD	[36]
Glass/MWCNT/papain	Protease assay	-	5 mg L^{-1}	2400	Human urine	CKD	[37]
TiO_2 nanobodies	Photoelectrochemical sensor	0.72 pM to 7.19 nM	0.14 pM	> 1200	Human serum	AKI	[38]
SPMWE/papain	Electrochemical immunosensor	0.6×10^{-5} to 0.6×10^{-2} ng μL^{-1}	0.5 ng L^{-1}	600	Urine	CKD	[12]
GCE/Fc-GO/PEI/anti-Cys	Electrochemical immunosensor	0.1 to 1000 ng mL^{-1}	0.03 ng mL^{-1}	-	Human serum	CKD	[13]
GCE/GO-Chit/anti-Cys	Electrochemical immunosensor	1–10 mg L^{-1}	0.0078 mg L^{-1}	420	Human serum	DR	Present work
SPE/GO-Chit/anti-Cys	Electrochemical immunosensor	1–10 mg L^{-1}	0.0026 mg L^{-1}	420	Human serum	DR	

GCE glassy carbon electrode, *DNA* deoxyribonucleic acid, *TiO_2* titanium oxide, *MWCNT* multiwalled carbon nanotubes, *anti-Cys* cystatin C antibody, *SPMWE* screen-printed multiwalled carbon working electrode, *Fc* ferrocene, *GO* graphene oxide, *Chit* chitosan, *PEI* polyethylenimine, *HPE* homemade screen-printed paper electrodes, *CKD* chronic kidney disorder, *AKI* acute kidney injury, *DR* diabetic retinopathy, *μUNPD* magnetic nanoparticle assay

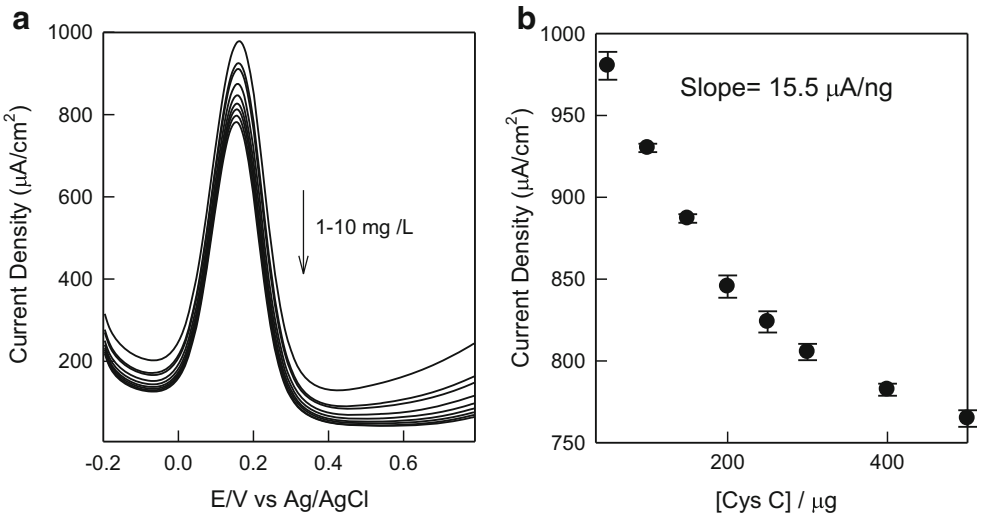

Fig. 5 DPV responses of the SPE integrated with 20-μL microfluidic chamber with modified GO-Chit@anti-Cys concentration effect and its calibration effect of the modified electrode (A, B) in 5 mM $Fe(CN)_6$ dissolved in pH 7 PBS

by standard addition approach, and the results are shown in Supplementary Fig. S4. Three different concentrations of Cys C were spiked in the sample and the recovery was between 85 and 90% ($n = 2$), exhibiting an excellent accuracy for the detection of Cys C in real samples. Table 1 shows the sensor prediction from actual samples which suggests that the GO-Chit-anti–Cys C has the potential to be developed as a reliable sensor for serum sample analysis.

It is seen from Table 1 that the sensor exhibits good accuracy (80%) in predicting the existence of diabetic retinopathy. However, the concentrations measured using ELISA and the sensor were different to predict DR status in the samples. This may be due to differences in the sample preparation and the measurement principle. Two of the control samples showed higher cystatin C levels when measured using the fabricated sensor which may be (a) due to interference with ascorbic acid or (b) due to existence of kidney disorders or associated disorders that may cause elevation in cystatin C levels. However, the sample size investigated is very less to draw any significant conclusion. Another trend that requires to be validated using a larger sample size is that the NPDR samples exhibit lower cystatin C values (< 2.3 mg/L) when compared with PDR. Whether this can be used to classify DR also can be arrived at only based on larger sample sizes.

The performance of the cystatin C sensor fabricated was compared with those of other reported cystatin C sensors (Table 2). It is seen that the modified glassy carbon electrode fabricated in the present study exhibits fast response time and has been used for predicting diabetic retinopathy in serum samples for the first time, whereas other sensors have used cystatin C as a biomarker for kidney disorders [12, 15, 34].

The promising results obtained using the modified GCE-GO-Chit-anti–Cys C electrode encouraged us to attempt to translate the modifications on a paper electrode platform to facilitate large-scale screening of diabetic population using affordable and disposable electrodes. The various modification steps carried out for the GCE were repeated with wax-coated paper substrate containing a screen-printed electrode pattern.

The modified paper electrode was placed in the microfluidic device and the various DPV parameters were optimized. The optimum amplitude, pulse widths, and increment E_{step} were 0.1 s, 0.02 s, and 0.05 s, respectively, which were similar to the optimized values from GCE. The active surface area of the paper electrode modified with GO-Chit-anti–Cys C was calculated to be 15.8×10^{-10} mol cm^{-2}. The electrode exhibited linearity between 1 and 10 mg/L of cystatin C (Fig. 5A) with a limit of detection of 2.6 pg/μL and sensitivity of 15.5 μA/ng (Fig. 5B). The detection limit was slightly better than those obtained on the GCE; however, the sensitivity was slightly reduced. A patient sample was tested with the given sensor, and based on the cystatin C concentration (1–10 mg/L) calculated from the current obtained, it was predicted that the sample belonged to a patient with DR which was found to be true. This correlated with the clinical diagnosis.

Concluding remarks

Overall, this study has resulted in the successful fabrication of an electrochemical cystatin C immunosensor with superior sensing parameters when compared with those reported in literature. The use of the graphene oxide-chitosan nanointerface enabled effective immobilization of the antibody as well as contributed to the higher sensitivity of the sensor. The sensor quantified cystatin C in the clinically relevant range and was validated using serum samples. The sensor was successfully used to predict the risk of diabetic retinopathy in patient samples for the first time, and the results showed a slightly better accuracy in prediction when compared with those obtained using the conventional ELISA technique. The same modifications were successfully reproduced in a paper electrode coupled with a microfluidic device designed in a 3D printing mould. The study has provided experimental

evidence that cystatin C could be a promising marker to predict diabetic retinopathy, and has developed an electrochemical immunosensor with disposable electrodes that could be integrated for making a simple device to screen diabetic population in future, with additional studies using a larger sample cohort.

Acknowledgements The authors thank SASTRA Deemed University for infrastructural support. We thank Dr. Sakthivel Gandhi and Ms. Sathiyasivam Kaviarasi for helping in the artwork of Scheme 1A and B. The authors also would like to thank SASTRA TBI (FIRST) for the use of 3D printing facilities.

Funding information The authors received funding from RCUK (grant number: MR/P027881/1).

Compliance with ethical standards

Conflict of interest The author(s) declare that they have no competing interests. All the experiments have been carried out in compliance with ethical standards in a prescribed format.

References

1. Chen X, Zhao S, Yu T, Zhang L, Li Q, Yu Y (2017) Serum cystatin C and chemerin levels in diabetic retinopathy. Int J Clin Exp Med 10:10827–10833
2. Wong CW, Teo BW, Lamoureux E, Ikram MK, Wang JJ, Tai ES, Sethi S, Wong TY, Sabanayagam C (2015) Serum cystatin C, markers of chronic kidney disease, and retinopathy in persons with diabetes. J Diabetes Res 2015:404280–404280
3. Chew JSC, Saleem M, Florkowski CM, George PM (2008) Cystatin C–a paradigm of evidence based laboratory medicine. Clin Biochem Rev 29(2):47–62
4. Finney H, Newman D, Price C (2000) Adult reference ranges for serum cystatin C, creatinine and predicted creatinine clearance. Ann Clin Biochem 37(Pt 1):49–59
5. Levy E (2012) Cystatin C in Alzheimer's disease, Front Mol Neurosci 5(79)
6. Gozashti MH, Gholamhosseinian A, Musavi F, Mashrouteh M (2013) Relationship between serum cystatin C and polycystic ovary syndrome. Iran J Reprod Med 11(1):71–76
7. Gowda S, Desai PB, Kulkarni SS, Hull VV, Math AAK, Vernekar SN (2010) Markers of renal function tests. N Am J Med Sci 2(4): 170–173
8. Ristiniemi N, Savage C, Bruun L, Pettersson K, Lilja H, Christensson A (2012) Evaluation of a new immunoassay for cystatin C, based on a double monoclonal principle, in men with normal and impaired renal function. Nephrol Dial Transplant 27(2): 682–687
9. Jiang R, Xu C, Zhou X, Wang T, Yao G (2014) Detection of cystatin C biomarker for clinical measurement of renal disease by developed ELISA diagnostic kits. J Transl Med 12:205–205
10. Tanaka M, Matsuo K, Enomoto M, Mizuno K (2004) A sol particle homogeneous immunoassay for measuring serum cystatin C. Clin Biochem 37(1):27–35
11. Yang ZH, Zhuo Y, Yuan R, Chai YQ (2016) Highly effective protein converting strategy for ultrasensitive electrochemical assay of cystatin C, (1520–6882 (Electronic))
12. Desai D, Kumar A, Bose D, Datta M (2018) Ultrasensitive sensor for detection of early stage chronic kidney disease in human. Biosens Bioelectron 105:90–94
13. Trindade EKG, Silva BVM, Dutra RF (2019) A probeless and label-free electrochemical immunosensor for cystatin C detection based on ferrocene functionalized-graphene platform. Biosens Bioelectron 138:111311
14. Zhao M, Bai L, Cheng W, Duan X, Wu H, Ding S (2019) Monolayer rubrene functionalized graphene-based eletrochemiluminescence biosensor for serum cystatin C detection with immunorecognition-induced 3D DNA machine. Biosens Bioelectron 127:126–134
15. Mi L, Wang P, Yan J, Qian J, Lu J, Yu J, Wang Y, Liu H, Zhu M, Wan Y, Liu S (2015) A novel photoelectrochemical immunosensor by integration of nanobody and TiO2 nanotubes for sensitive detection of serum cystatin C, Analytica Chimica Acta 902
16. Mohammadi S, Busa LSA, Maeki M, Mohamadi RM, Ishida A, Tani H, Tokeshi M (2016) Rapid detection of cat cystatin C (cCys-C) using immuno-pillar chips. Anal Sci 32(12):1359–1362
17. Lee J, Kim J, Kim S, Min D-H (2016) Biosensors based on graphene oxide and its biomedical application. Adv Drug Deliv Rev 105:275–287
18. Gong X, Bi Y, Zhao Y, Liu G, Teoh WY (2014) Graphene oxide-based electrochemical sensor: a platform for ultrasensitive detection of heavy metal ions. RSC Adv 4(47):24653–24657
19. Xu L, Wen Y, Pandit S, Mokkapati VRSS, Mijakovic I, Li Y, Ding M, Ren S, Li W, Liu G (2019) Graphene-based biosensors for the detection of prostate cancer protein biomarkers: a review. BMC Chem 13(1):112–112
20. Pauliukaite R, Ghica ME, Fatibello-Filho O, Brett CMA (2009) Comparative study of different cross-linking agents for the immobilization of functionalized carbon nanotubes within a chitosan film supported on a graphite–epoxy composite electrode. Anal Chem 81(13):5364–5372
21. Ibáñez-Redín, Materon EM, Furuta RHM, Wilson D, do Nascimento GF, Melendez ME, Carvalho AL, Reis RM, Oliveira ON, Gon alves D (2020) Screen-printed electrodes modified with carbon black and polyelectrolyte films for determination of cancer marker carbohydrate antigen 19-9. Microchimica Acta 187(7):417
22. Wongkaew P, Poosittisak S (2016) Atomic force microscopic and electrochemical characterization of the modified screen printed carbon electrode by self assembled deposition of chitosan and activated carbon. Int J Geomate 11:2356–2362
23. Archana S, Kumar KY, Jayanna BK, Olivera S, Anand A, Prashanth MK, Muralidhara HB (2018) Versatile graphene oxide decorated by star shaped zinc oxide nanocomposites with superior adsorption capacity and antimicrobial activity. J Sci Adv Mater Devices 3(2):167–174
24. Patra P, Mitra S, Debnath N, Pramanik P, Goswami A (2014) Ciprofloxacin conjugated zinc oxide nanoparticle: a camouflage towards multidrug resistant bacteria. Bull Mater Sci 37(2):199–206
25. Shobha Jeykumari DR, Ramaprabhu S, Sriman Narayanan S (2007) A thionine functionalized multiwalled carbon nanotube modified electrode for the determination of hydrogen peroxide. Carbon 45(6):1340–1353
26. Sun W, Zhang Y, Ju X, Li G, Gao H, Sun Z (2012) Electrochemical deoxyribonucleic acid biosensor based on carboxyl functionalized graphene oxide and poly-l-lysine modified electrode for the detection of tlh gene sequence related to vibrio parahaemolyticus. Anal Chim Acta 752:39–44
27. Kang X, Wang J, Wu H, Aksay IA, Liu J, Lin Y (2009) Glucose oxidase–graphene–chitosan modified electrode for direct electrochemistry and glucose sensing. Biosens Bioelectron 25(4):901–905
28. Li Z, Wang W, Ding C, Wang Z, Liao S, Li C (2017) Biomimetic electron transport via multiredox shuttles from photosystem II to a photoelectrochemical cell for solar water splitting. Energy Environ Sci 10(3):765–771
29. Natarajan A, Devi KSS, Raja S, Senthil Kumar A (2017) An elegant analysis of white spot syndrome virus using a graphene oxide/

methylene blue based electrochemical immunosensor platform. Sci Rep 7(1):46169
30. Brazaca LC, Ribovski L, Janegitz BC, Zucolotto V (2017) 10 - Nanostructured materials and nanoparticles for point of care (POC) medical biosensors, in: R.J. Narayan (Ed.), Medical biosensors for point of care (POC) applications, Woodhead Publishing, pp. 229–254
31. Hussain G, Silvester DS (2016) Comparison of voltammetric techniques for the electroanalysis of dissolved solids and gases in water, acetonitrile and room temperature ionic liquids (RTILs): unusual behaviour for gases, Meeting Abstracts MA2016–02(46) 3403–3403
32. Shalini Devi KS, Mahalakshmi VT, Ghosh AR, Kumar AS (2017) Unexpected co-immobilization of lactoferrin and methylene blue from milk solution on a Nafion/MWCNT modified electrode and application to hydrogen peroxide and lactoferrin biosensing. Electrochim Acta 244:26–37
33. Liu Q, Wang H, Li H, Zhang J, Zhuang S, Zhang F, Jimmy Hsia K, Wang P (2013) Impedance sensing and molecular modeling of an olfactory biosensor based on chemosensory proteins of honeybee. Biosens Bioelectron 40(1):174–179
34. Psychogios N, Hau DD, Peng J, Guo AC, Mandal R, Bouatra S, Sinelnikov I, Krishnamurthy R, Eisner R, Gautam B, Young N, Xia J, Knox C, Dong E, Huang P, Hollander Z, Pedersen TL, Smith SR, Bamforth F, Greiner R, McManus B, Newman JW, Goodfriend T, Wishart DS (2011) The human serum metabolome. PLoS One 6(2): e16957–e16957
35. Mohammadi S, Busa LS, Maeki M, Mohamadi RM, Ishida A, Tani H, Tokeshi M. Rapid detection of cat cystatin C (cCys-C) using immuno-pillar chips, (1348–2246 (Electronic))
36. Chung HJ, Pellegrini KL, Chung J, Wanigasuriya K, Jayawardene I, Lee K, Lee H, Vaidya VS, Weissleder R (2015) Nanoparticle detection of urinary markers for point-of-care diagnosis of kidney injury. PLoS One 10(7):e0133417
37. Datta D, John Stephen B, Desai D (2017) An alternative diagnostic design for chronic kidney disease detection based on cystatin C. Asian J Pharm Clin Res 10:425
38. Mi L, Wang P, Yan J, Qian J, Lu J, Yu J, Wang Y, Liu H, Zhu M, Wan Y, Liu S (2016) A novel photoelectrochemical immunosensor by integration of nanobody and TiO2 nanotubes for sensitive detection of serum cystatin C. Anal Chim Acta 902:107–114